ISSN: 2579-5821 (Print)
ISSN: 2579-5546 (Online)
URL address: http://journal.unhas.ac.id/index.php/geocelebes
DOI: 10.70561/geocelebes.v10i1.48347

Jurnal Geocelebes Vol. 10 No. 1, April 2026, 12 – 33

Analysis of Flood Vulnerability and Rainfall Changes in the Angke-Pesanggrahan Watershed using Spatial Mapping

Ratu Kenanga Fitria*, Yayat Ruhiat, Yuvita Oktarisa

Physics Education, Sultan Ageng Tirtayasa University, Serang, 42117, Indonesia.

*Corresponding author. Email: 2280220023@untirta.ac.id

Manuscript received: 16 November 2025; Received in revised form: 31 December 2025; Accepted: 31 Januari 2026

Abstract

This study analyzes flood vulnerability in the Angke-Pesanggrahan Watershed, Jakarta, which faces increased risks due to land-use changes. The study aims to calculate the 50-year return period flood discharge, map flood-prone zones, and formulate mitigation recommendations using spatial mapping. A quantitative approach was employed, analyzing 15 years of rainfall data from five stations. Methodology included data consistency testing, Spearman's correlation, stationarity, and outlier identification, followed by regional rainfall analysis using Thiessen Polygons. The Log Pearson Type III distribution was applied for frequency analysis, and the Nakayasu Synthetic Unit Hydrograph method estimated flood discharge. Flood-prone zones were mapped using scoring and overlay techniques in a Geographic Information System (GIS). Results show that the 50-year flood discharge reaches 1.128 m^3/s, exceeding existing river capacity. Mapping simulations identified flood depths of 3–6 meters in downstream areas, with high-risk zones concentrated in Northern Kembangan, Kedaung Kali Angke, Kapuk Muara, Kamal Muara, Eastern Cengkareng, and Northern Kedoya, where surface runoff contributes up to 90%. Spatial analysis categorized 257.18 km^2 as non-prone, 92.14 km^2 as moderately prone, 75.75 km^2 as prone, and 58.57 km^2 as highly prone. This study concludes that the Angke-Pesanggrahan Watershed, particularly the Cengkareng Drain section, requires urgent technical intervention, including river normalization and catchment area optimization. These findings provide a crucial spatial database for sustainable flood mitigation and risk-based decision-making in urban planning.

Keywords: Angke-Pesanggrahan Watershed; Disaster Mitigation; Nakayasu HSS; Q50 Flood Discharge; Spatial Mapping.

Citation: Fitria, R. K., Ruhiat, Y., & Oktarisa, Y. (2026). Analysis of Flood Vulnerability and Rainfall Changes in the Angke-Pesanggrahan Watersheds using Spatial Mapping. *Jurnal Geocelebes*, 10(1): 12–33, doi: 10.70561/geocelebes.v10i1.48347

Introduction

Flood vulnerability in the Angke-Pesanggrahan River Basin, particularly in Jakarta, has increased in line with population growth and massive land use changes (Habibi & Darmawan, 2024). Land conversion reduces soil absorption and river retention capacity, causing frequent surface runoff and annual flooding in downstream areas such as North Kembangan-Kamal Muara (Ignes & Arbaningrum, 2021). BNPB data from 2015 recorded 93 flood points in Jakarta (Novarini et al., 2024), while regional development has significantly altered the land cover in the Pesanggrahan watershed, leading to a substantial increase in surface runoff where urbanized areas now contribute to a higher percentage of immediate flood discharge rather than natural infiltration (Taki & Wartaman, 2022). As a result, a 3.5 meter flood hit Pesanggrahan in 2025, causing hundreds of residents to evacuate (Abdolazimi et al., 2025; Noviansah, 2025) and blocking several roads in Kembangan, West Jakarta (Syukur, 2025).

© 2026 Dept. of Geophysics Hasanuddin University

A review of previous studies shows significant developments in flood modelling, but there is still room for further discussion and exploration. Habibi & Darmawan (2024), Mitu et al. (2025) and Limeria & Saputra (2024) have successfully applied the HEC-RAS model (1D and 2D) to predict peak discharge and inundation area at various return periods, but their analysis tends to focus on hydraulic dynamics within river channels without integrating broad physical land variables. On the other hand, Fox et al. (2024) and Sinurat et al. (2022) have gone further by converting HEC-RAS output into spatial format using QGIS and InaSAFE for economic loss analysis, but the vulnerability parameters used do not yet cover detailed biophysical characteristics of the soil. A research gap exists in the lack of integration between design discharge (Q_{50}) and multifactorial geospatial parameters that determine water retention capacity outside the river channel. This study aims to fill this gap by developing a more comprehensive flood vulnerability mapping approach through scoring and overlay techniques on seven key parameters, which are rainfall intensity, administrative boundaries, soil infiltration, land slope, elevation, land use, and soil texture. The strength of this study lies in the cross-validation between Nakayasu's Synthetic Unit Hydrograph (HSS) hydrological modelling, HEC-RAS 6.7 hydraulic simulation, and geospatial mapping from the Geospatial Information Agency, in order to map hotspots of vulnerability in the Angke-Pesanggrahan watershed more precisely amid massive trends in climate change and land use. The study was conducted in the Angke-Pesanggrahan watershed, Jakarta, as shown in the location map in Figure 1.

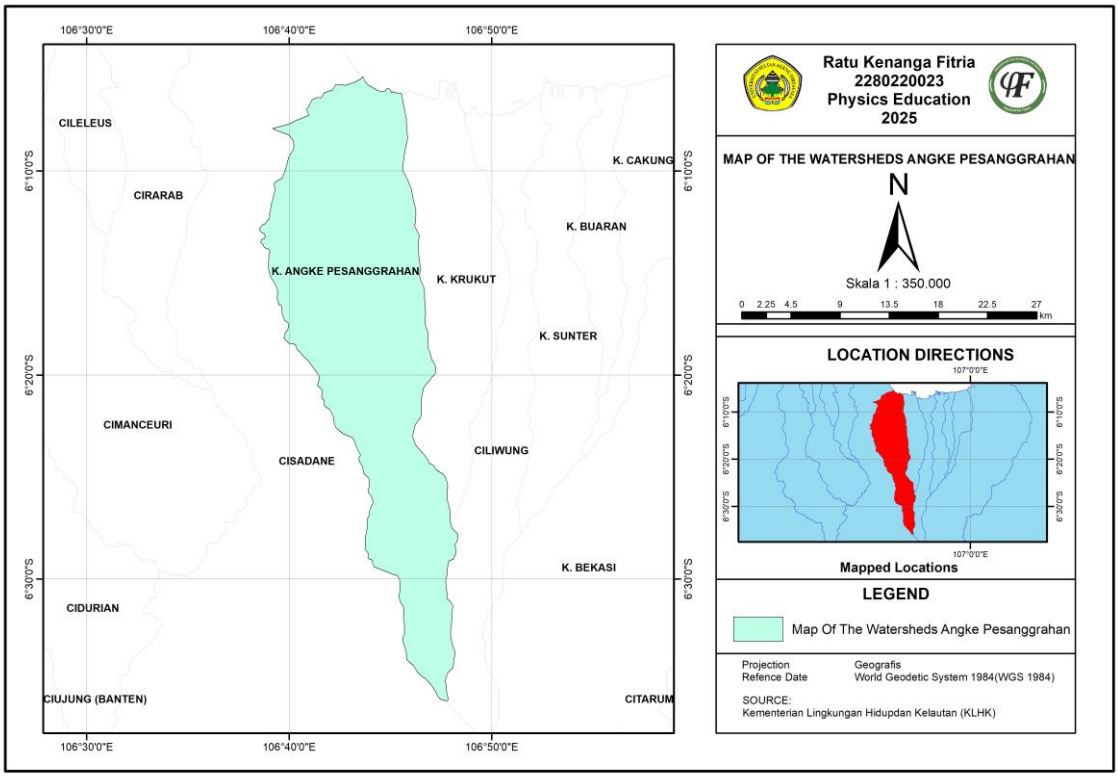

Figure 1. Angke-Pesanggrahan watersheds map.

Materials and Methods

Regional Geology and Research Area

Watersheds are vital areas for the preservation of the water cycle. Topographically, a watershed functions as a catchment area that collects and carries

© 2026 Dept. of Geophysics Hasanuddin University

rainwater runoff through river systems to lower areas or the sea (Dahlia & Fadiarman, 2020). This area is an ecological system where natural components such as soil, water, and vegetation interact with human activities, particularly in densely populated regions where land-use changes significantly affect the hydrological balance and increase flood risks (Taki & Wartaman, 2022). These characteristics significantly influence the hydrological response and flow patterns within the watershed when subjected to rainfall (Yu et al., 2025; Rhianazala et al., 2026). In tropical regions like Indonesia, atmospheric conditions often lead to high-intensity rainfall events that exceed drainage capacities. Recent spatial analyses in Greater Jakarta demonstrate that extreme rainfall intensity, coupled with topographic factors, remains a primary driver of urban flood vulnerability, often resulting in rapid surface runoff and significant hazard zones (Muhammad et al., 2025). The geographical locations of the five rainfall stations used in this study, including their coordinates, are detailed in Table 1.

Table 1. Location of Rainfall Stations in the Angke-Pesanggrahan watershed (PSDA WS Ciliwung-Cisadane, 2019).

No	Rain Station	Geographical Location	
		Latitude	Longitude
1	Sawangan	06° 18’ 54.4’’ S	106° 45’ 51.2’’ E
2	Bendung Gintung	06° 34’ 28.9’’ S	106° 52’ 58.6’’ E
3	Cengkareng Drain	06° 09’ 13.3’’ S	106° 44’ 52.6’’ E
4	Situ Parigi	06° 16’ 53.6’’ S	106° 41’ 48.3’’ E
5	Villa Pamulang	06° 20’ 34.6’’ S	106° 43’ 22.8’’ E

Data Collection

This study uses one sources of information; this secondary data came from the Ciliwung-Cisadane River Basin Management Agency and the Geospatial Information Agency. The secondary data obtained is as follows:

1.) Daily rainfall data from the Sawangan Rainfall Station, Bendung Gintung, Cengkareng, Situ Parigi, and Villa Pamulang for 15 years.
2.) Administrative boundary data West Java, DKI Jakarta, and Banten Province.
3.) Land cover data for West Java, DKI Jakarta, and Banten Province.
4.) Elevation data, land slope, soil drainage, soil texture of West Java province, DKI Jakarta, and Banten.

Analysis of Extreme Rainfall

The frequency analysis in this study was performed using the Log Pearson Type III distribution to estimate extreme rainfall events. This method is highly recommended for hydrological modelling in tropical regions due to its flexibility in handling skewed data distribution (Abdolazimi et al., 2025; Ismael & Awchi, 2023) Rainfall frequency analysis was performed using the Log Pearson Type III distribution, which is the standard approach for analyzing hydrological extreme values in tropical regions (Guo et al., 2025), as shown in Equation (1).

$$log\ \ X = \overline{LogX} + k(\overline{S\ log\ X}) \qquad (1)$$

where:
$\overline{LogX}$: mean value of log X.
k : frequency factor (found in the Pearson III table).
$\overline{S\ log\ X}$: standard deviation of log X.

Rainfall in the Region Thiessen Polygon Method

The regional average rainfall is determined by considering the spatial distribution of observation points, where the Thiessen Polygon method is applied to assign area-weighting factors to each station (Kwak et al., 2024; Rahmadani et al., 2023). The regional average rainfall was estimated by

© 2026 Dept. of Geophysics Hasanuddin University

applying the area-weighting formula shown in Equation (2). The regional average rainfall was calculated using the Thiessen Polygon spatial interpolation method to account for the uneven distribution of rain gauges (Dahlia & Fadiarman, 2020):

$$\bar{R} = \frac{A_1R_1+A_2R_2+I+A_nR_n}{A_1+A_2+I+A_n} \quad (2)$$

with:
$\bar{R}$: Average rainfall in the area (mm).
A_1, A_2, A_n : Area represented by each observation point (m^2).
R_1, R_2, R_n : Rainfall at observation location 1 (mm).

The spatial distribution and influence area of each rainfall station were determined using the Thiessen Polygon method, which ensures a representative average rainfall calculation for the entire watershed.

Debit Analysis Flood (Nakayasu HSS)

The peak flood discharge for the 50-year return period was estimated using the Nakayasu Synthetic Unit Hydrograph (SUH) method, as formulated in Equation (3). To estimate peak flood discharge, the Nakayasu SUH was applied, as it is calibrated for Indonesian watershed characteristics (Rahmadani et al., 2024).

$$Q_p = \frac{A \times R_0}{3{,}6(0{,}3T_p+T_{0,3})} \quad (3)$$

The calculation of river dimensions is based on the discharge that must be accommodated by the river (Q_s), which is greater than or equal to the planned discharge (Q_T) influenced by planned rainfall (R_T). To evaluate whether the existing river can accommodate the flood, the hydraulic capacity of the river channel was evaluated using Manning's equation to determine the threshold for overtopping during peak discharge, the cross-sectional capacity was analyzed using Equation (4) and Equation (5). One way to describe this condition is as follows (Setiyawan et al., 2022; Taki & Wartaman, 2022):

$$Q_s > Q_T \quad (4)$$

The discharge that can be accommodated by the river (Q_s) is obtained using the following formula:

$$Q_s = A_S V \quad (5)$$

Formula explanation:
A_s : Wet cross-sectional area of the river (m^2).
V : Average flow velocity according to material type (m/s).

To transform effective rainfall into flood hydrographs, the Nakayasu SUH was employed. This approach has been widely validated for urban watersheds in Indonesia to accurately predict peak discharge timing and volume (Handore et al., 2025).

Spatial Mapping Flood Vulnerability

Accuracy testing of spatial mapping was conducted using the cross-validation method by comparing ArcGIS spatial output parameters with actual accumulation data from HEC-RAS numerical modelling. The accuracy of vulnerability maps was measured based on the consistency between spatially defined 'Highly Vulnerable' zones and hydrodynamic parameters at relevant river stations.

Scoring

Vulnerability scores are calculated by multiplying the relative weight of each criterion with its corresponding rank value, a method known as Weighted Overlay Analysis (Soma et al., 2021). The scoring system for each physical parameter, such as land use, rainfall, slope, and soil characteristics, is defined in Table 2 – 7, while the assigned weights are shown in Table 8.

Table 2. Scores for land closure classes (Alif et al., 2025).

No	Class	Score
1	Rice fields, open land	9
2	Dry fields, settlements	7
3	Bushes, thickets, reeds	5
4	Plantations	3
5	Forests	1
6	Clouds and shadows	1

© 2026 Dept. of Geophysics Hasanuddin University

Table 3. Scores for rainfall classes (Alif et al., 2025).

No	Class	Score
1	> 3000 mm (very wet)	9
2	2501 – 3000 mm (wet)	7
3	2001 – 2500mm (moderately damp)	5
4	1502 – 2000 mm (dry)	3
5	< 1500mm (very dry)	1

Table 4. Score for land slope classes (Alif et al., 2025).

No	Class	Score
1	Flat (0 – 3%)	9
2	Undulating (3 – 8%)	7
3	Wavy (8 – 15%)	5
4	Small hills (15 – 30%)	3
5	Hills (30 – 45%)	1
6	Steep hills (> 45%)	0

Table 5. Scores for the upper grades (Allafta & Opp, 2021).

No	Class	Score
1	0 – 12.5m	9
2	12.5 – 25m	7
3	25 – 50m	5
4	50 – 75m	3
5	75 – 100m	1
6	> 100m	0

Table 6. Score for soil texture classes (Alif et al., 2025).

No	Class	Score
1	Very smooth	9
2	Smooth	7
3	Medium	5
4	Rough	3
5	Very rough	1

Table 7. Score for soil drainage classes (Endendijk et al., 2023).

No	Class	Score
1	Hindered	9
2	Somewhat hindered	7
3	Somewhat hindered – Moderate	5
4	Moderate	3
5	Fast	1

Table 8. Weight of parameters causing flooding (Alif et al., 2025).

No	Parameter	Weight
1	Land slope	0.2
2	Elevation class	0.1
3	Soil texture	0.2
4	Soil permeability (drainage)	0.1
5	Rainfall	0.15
6	Land use	0.15
7	River buffer	0.1

Overlay

This stage involves combining all parameters using overlay weight sum (Saad et al., 2024). The score attributes of each parameter will be overlaid to produce a new layer, thereby automatically calculating the score.

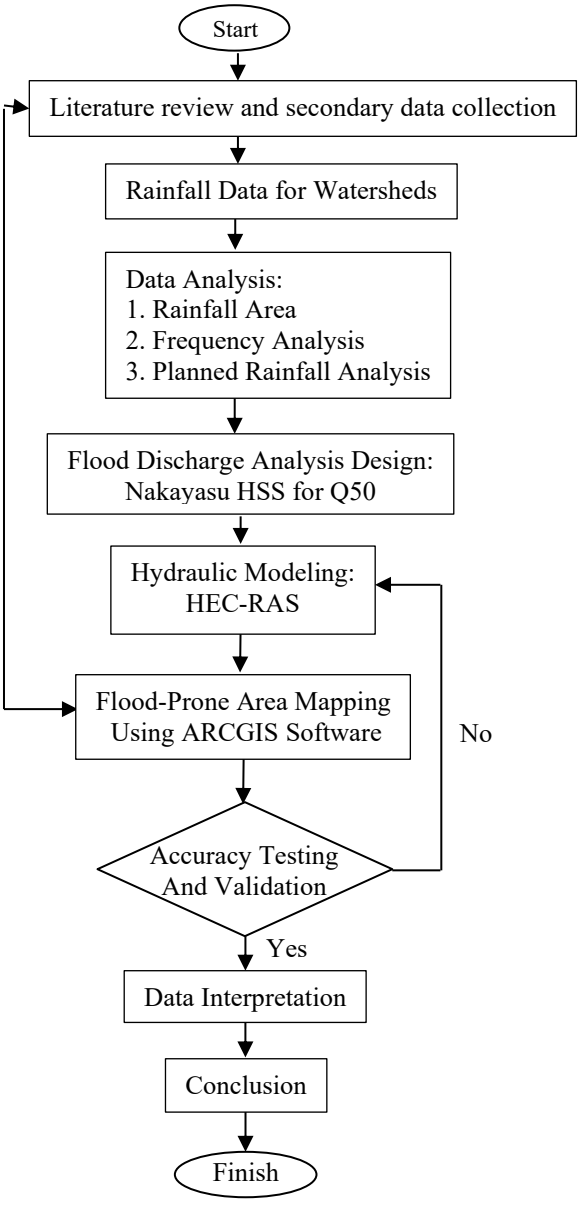

Figure 2. Flowchart of research analysis of flood vulnerability in the Angke-Pesanggrahan watershed spatial mapping and rainfall changes.

Reclassification of flood vulnerability levels

This stage involves classifying the overlay results separated into four groups of vulnerability: safe, not vulnerable, moderately vulnerable, and highly vulnerable.

© 2026 Dept. of Geophysics Hasanuddin University

The systematic workflow of this research, from data collection to final mapping, is depicted in the flowchart in Figure 2.

Results and Discussion

Rainfall Plan

Extreme price distribution

In this study, the Maximum Annual Series Method was used to ensure that there was only one data point per year, representing the maximum average rainfall value available for each period. This approach is essential for establishing a consistent dataset for flood susceptibility and vulnerability modelling (Safaei-moghadam et al., 2024). The recorded maximum daily rainfall data and the completed dataset used for further analysis are presented in Table 9 – 11.

Table 9. Maximum Daily Rainfall Data (PSDA WS Ciliwung-Cisadane, 2023).

Year	Sawangan	Bendung Gintung	Cengkareng Drain	Situ Parigi	Villa Pamulang
	Daily P (mm)				
2009	85	0	139	0	0
2010	108	0	75	0	0
2011	76	0	83	0	0
2012	83.4	0	54	0	0
2013	100	0	91	0	0
2014	100	0	105	0	0
2015	43.6	50	124	0	0
2016	105	95	120	0	0
2017	39.8	105.5	110	0	0
2018	60	67.5	83	0	0
2019	135	135	423	158	112
2020	50.7	0	156	175	94.5
2021	92	134	92.5	122.3	83.5
2022	98.4	122.5	124.5	157	85
2023	116.5	82	62	89	88

Table 10. Missing rainfall.

Year	Sawangan	Bendung Gintung	Cengkareng Drain	Situ Parigi	Villa Pamulang
	Daily P (mm)				
2009	85	0	139	0	0
2010	108	0	75	0	0
Total	1293.4	791.5	1842	701.3	463

Normal Ratio Method

The calculation used is quite simple, which is by calculating rainfall data at nearby rain stations to find the missing rainfall data at that station. The variables in this method are the daily rainfall at other stations and the total rainfall for 1 year at those other stations. For 2009, the table is on Table 10.

Table 11. Complete rainfall data (mm).

Year	Sawangan	Bendung Gintung	Cengkareng Drain	Situ Parigi	Villa Pamulang
	Daily P (mm)				
2009	85	27.9	139	30.9	25.5
2010	108	24.6	75	27.2	22.5
2011	76	20.5	83	22.8	18.8
2012	83.4	18.6	54	20.6	17
2013	100	25.1	91	27.8	22.9
2014	100	26.6	105	29.4	24.3
2015	43.6	50	124	28.8	23.8
2016	105	95	120	46.7	38.5
2017	39.8	105.5	110	39.2	32.4
2018	60	67.5	83	31	25.6
2019	135	135	423	158	112
2020	50.7	114.3	156	175	94.5
2021	92	134	92.5	122.3	83.5
2022	98.4	122.5	124.5	157	85
2023	116.5	82	62	89	88

Using the Normal Ratio formula, we get:

$$d_x = \frac{1}{n}\sum_{t=1}^{n} d_i \frac{An_x}{An_i}$$

$$d_x = \frac{1}{4}(139 \times \frac{791.5}{1842} + 85 \times \frac{791.5}{1293.5} + 0 \times \frac{791.5}{701.3} + 0 \times \frac{791.5}{463})$$

$$d_x = 27.94 \text{ mm}$$

The same applies to other years, with the following results.

Double period curve consistency test

Before collecting data, it is important to understand the nature of the data that will be used in the study. The consistency test results at each station are quite good, the reliability of the rainfall data was verified through a double-mass curve consistency test, as shown in the graphs in Figure 3.

Based on the analysis results, the validation of rainfall data feasibility for flood discharge analysis is reinforced by comprehensive statistical test findings. Furthermore, the application of double-mass curve consistency testing is a fundamental prerequisite to ensure the reliability and integrity of the hydrological

© 2026 Dept. of Geophysics Hasanuddin University

data before integrating multiple criteria into the subsequent discharge calculations and spatial analysis (Bahago et al., 2026). The results of double mass curve consistency testing show a stable and homogeneous rainfall accumulation pattern across all stations, proving that historical data is highly reliable for flood vulnerability analysis. The stability of this trend reflects the influence of regional meteorological phenomena such as La Niña, which periodically triggers extreme rainfall in the Greater Jakarta area but is still recorded consistently between stations without any systematic errors in the measuring instruments. These findings are in line with a previous study (Wigati & Wahyudin, 2013) on the characteristics of extreme rainfall in Jakarta, where spikes in accumulation on the double mass curve coincide with periods of regional climate anomalies. Thus, the consistency of this data provides an accurate climate information base for spatial mapping of flood-affected areas in the Angke-Pesanggrahan watershed.

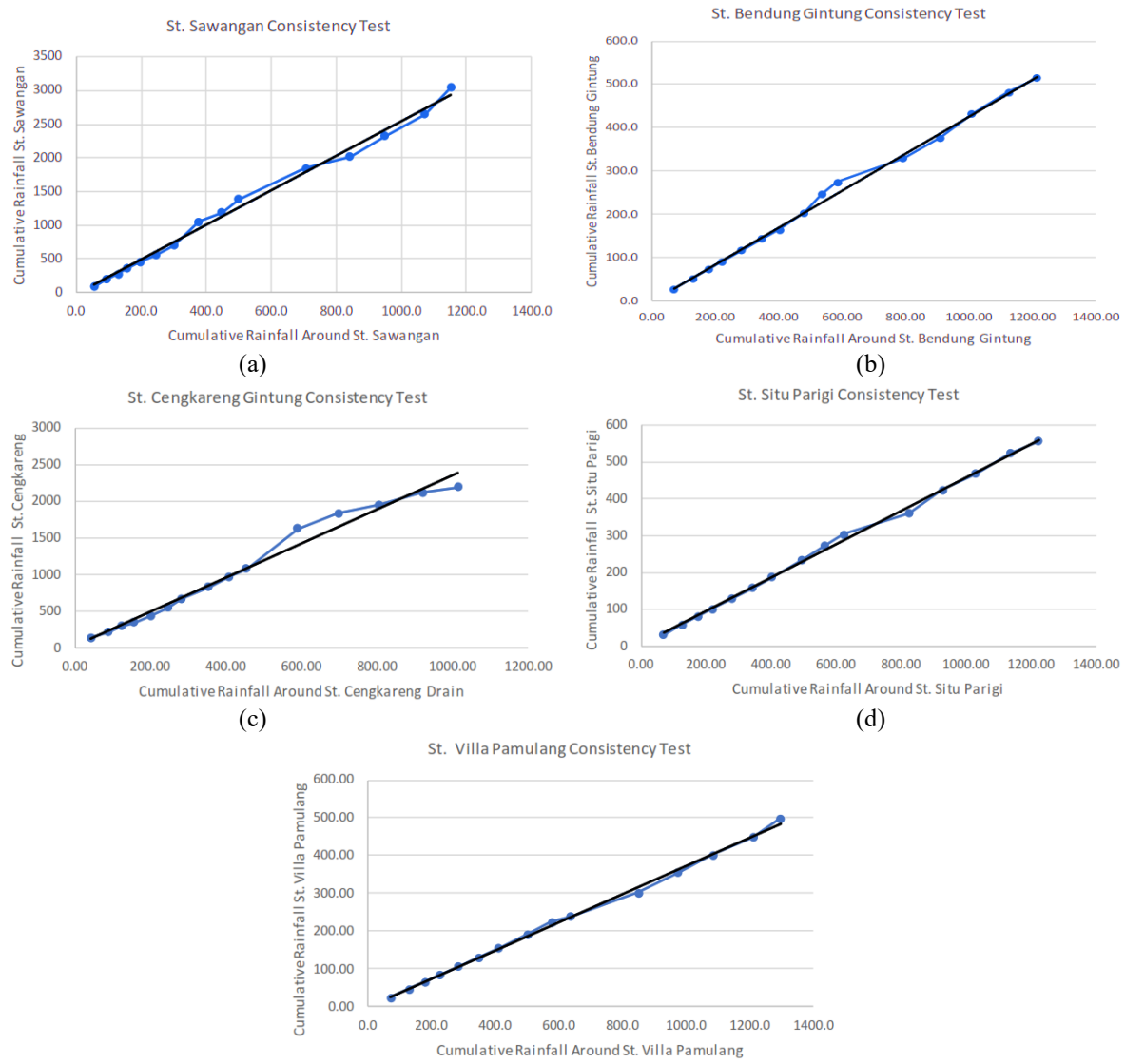

Figure 3. Data Consistency Graph (a) Sawangan Station, (b) Bendung Gintung Station, (c) Cengkareng Drain Station, (d) Situ Parigi Station, (e) Villa Pamulang Station.

Furthermore, about data stationarity, which in this study was proven through F-tests and T-tests showing variance and mean stability, is a critical assumption in

© 2026 Dept. of Geophysics Hasanuddin University

hydrological frequency analysis. Support also comes from Muhammad et al. (2025), who emphasizes that rainfall data with non-trend and non-persistent characteristics, identified through Spearman and Cox-Stuart tests, provide a valid basis for flood modelling in urban areas such as the Angke-Pesanggrahan River Basin.

The reliability of the rainfall dataset was ensured by conducting an outlier test and consistency check before the simulation. This preprocessing step is crucial to eliminate anomalies that could potentially bias the hydraulic simulation results (Carr et al., 2025; Mester et al., 2025; Saraswati et al., 2023).

Table 12. Results of rainfall data analysis calculations for the Sawangan station.

Testing	α	Zm/F/T	Zcr/Fcr/tcr	Conclusion	
Spearman Trend Absence Test	5%	-4,96	1,771	-Zcr < Z < Zcr	There is no trend
Cox and Stuart Trend Absence Test	1%	1,78	2,58	-Zcr < Z < Zcr	There is no trend
Cox and Stuart Trend Absence Test	5%	1,789	1,96	-Zcr < Z < Zcr	There is no trend
Stationarity Test (F-test)	5%	0,04	4,28	F < Fcr	Stable Variation
Stationarity Test (T-test)	5%	-24,6	1,78	-tcr < t < tcr	Stable Average
Spearman Persistence Test	5%	2,44	1,771	-tcr < t	Dependence Data

Table 13. Results of rainfall data analysis calculations for the Bendung Gintung station.

Testing	α	Zm/F/T	Zcr/Fcr/tcr	Conclusion	
Spearman Trend Absence Test	5%	-3,88	1,771	-Zcr < Z < Zcr	There is no trend
Cox and Stuart Trend Absence Test	1%	1,78	2,58	-Zcr < Z < Zcr	There is no trend
Cox and Stuart Trend Absence Test	5%	1,78	1,96	-Zcr < Z < Zcr	There is no trend
Stationarity Test (F-test)	5%	0,13	4,28	F < Fcr	Stable Variation
Stationarity Test (T-test)	5%	-33,9	1,78	-tcr < t < tcr	Stable Average
Spearman Persistence Test	5%	2,22	1,77	-tcr < t	Dependence Data

Table 14. Results of rainfall data analysis calculations for the Cengkareng station.

Testing	α	Zm/F/T	Zcr/Fcr/tcr	Conclusion	
Spearman Trend Absence Test	5%	-1,76	1,77	-Zcr < Z < Zcr	There is no trend
Cox and Stuart Trend Absence Test	1%	0.89	2,58	-Zcr < Z < Zcr	There is no trend
Cox and Stuart Trend Absence Test	5%	0,89	1,96	-Zcr < Z < Zcr	There is no trend
Stationarity Test (F-test)	5%	0,04	4,28	F < Fcr	Stable Variation
Stationarity Test (T-test)	5%	-11,2	1,78	-tcr < t < tcr	Stable Average
Spearman Persistence Test	5%	0,78	1,77	t < tcr	Random Data

Table 15. Results of rainfall data analysis calculations for the Situ Parigi station.

Testing	α	Zm/F/T	Zcr/Fcr/tcr	Conclusion	
Spearman Trend Absence Test	5%	-4,27	1,77	-Zcr < Z < Zcr	There is no trend
Cox and Stuart Trend Absence Test	1%	1,789	2,58	-Zcr < Z < Zcr	There is no trend
Cox and Stuart Trend Absence Test	5%	1,789	1,96	-Zcr < Z < Zcr	There is no trend
Stationarity Test (F-test)	5%	0,11	4,28	F < Fcr	Stable Variation
Stationarity Test (T-test)	5%	-28,9	1,78	-tcr < t < tcr	Stable Average
Spearman Persistence Test	5%	2,9	1,77	-tcr < t	Dependence Data

Table 16. Results of rainfall data analysis calculations for the Villa Pamulang station.

Testing	α	Zm/F/T	Zcr/Fcr/tcr	Conclusion	
Spearman Trend Absence Test	5%	-3,4	1,77	-Zcr < Z < Zcr	There is no trend
Cox and Stuart Trend Absence Test	1%	1,789	2,58	-Zcr < Z < Zcr	There is no trend
Cox and Stuart Trend Absence Test	5%	1,789	1,96	-Zcr < Z < Zcr	There is no trend
Stationarity Test (F-test)	5%	0,04	4,28	F < Fcr	Stable Variation
Stationarity Test (T-test)	5%	-21,3	1,78	-tcr < t < tcr	Stable Average
Spearman Persistence Test	5%	1,06	1,77	t < tcr	Random Data

The analysis of rainfall characteristics across the five stations shows varied yet statistically consistent results. Based on the data presented in Table 12, 13, and 15, the

© 2026 Dept. of Geophysics Hasanuddin University

calculated values for Sawangan, Bendung Gintung, and Situ Parigi stations exceed the critical value at α = 5%, confirming the persistent nature or serial dependence of the data. Conversely, the test results in Table 14 and 16 show that data fluctuations remain within stationary limits through F-tests and T-tests. This demonstrates that, overall, the rainfall data does not experience extreme shifts in mean or variance over time.

The data validity Is further supported by the outlier test results shown in Figure 4. Although the Saluran Cengkareng station shows data points exceeding the outlier threshold, these values are considered reasonable and hydrologically acceptable as they do not deviate significantly from historical trends. Consequently, the entire dataset is declared valid for use as input in the planned rainfall frequency analysis using the Log Pearson Type III distribution.

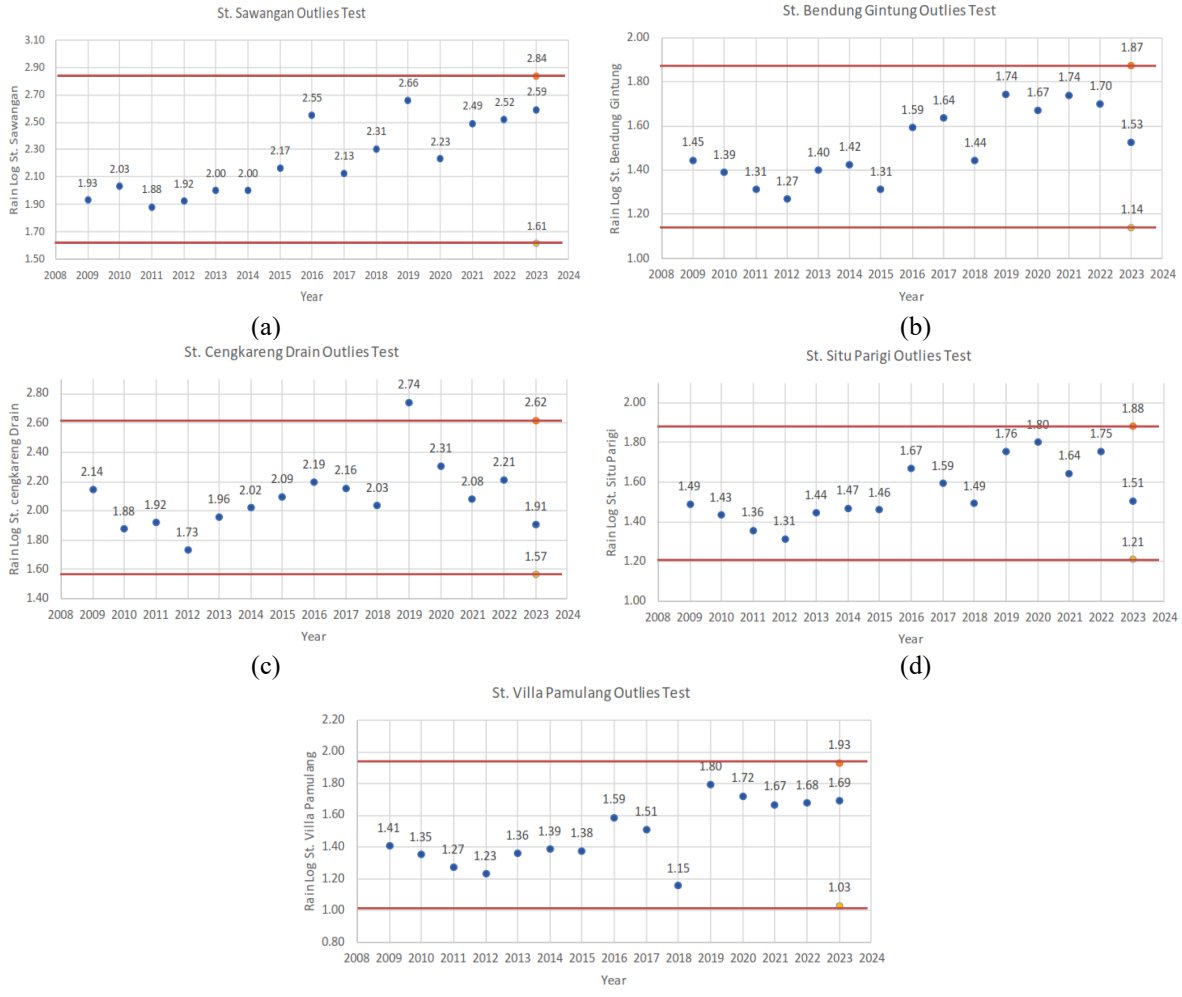

Figure 4. Outlier test graph (a) Sawangan Station, (b) Bendung Gintung Station, (c) Cengkareng Drain Station, (d) Situ Parigi Station, € Villa Pamulang Station.

The stability of data without trends reflects that despite annual fluctuations, long-term hydrological characteristics in this region remain consistent for use in modelling. In terms of regional meteorology, the absence of trends indicates that rainfall spikes are periodic, influenced by the La Niña phenomenon, which historically triggers extreme rainfall anomalies in Jakarta without permanently changing long-term distribution patterns. Compared to previous studies on extreme rainfall in the Angke-Pesanggrahan watershed, the recorded extreme values including outliers at the Cengkareng Drain Station—are representative of the high rainfall intensity

© 2026 Dept. of Geophysics Hasanuddin University

typical of regional climate anomalies and are not systematic errors. These outliers were not eliminated from the dataset because their positions were still within the main distribution threshold, in line with the approach taken by Glas et al. (2023).

The existence of stable and stationary extreme data is crucial input for HEC-RAS modelling, where the resulting design rainfall triggers a peak discharge (Q_{50}) of 1127.97 m^3/s. This figure is validated as a critical condition for river capacity, where the numerical profile shows that the water level reaches 4.15 m, which directly explains the mechanical cause behind the spatial distribution of flood vulnerability mapped through ArcGIS.

Area Rainfall

In terms of rainfall areas, rainfall stations are located in designated Watershed Areas (DAS), although they can also be found in adjacent DAS. Five rainfall stations are located within the Angke Pesanggrahan Watershed, which are Sawangan Station, Bendung Gintung Station, Situ Parigi Station, Villa Pamulang Station, and Cengkareng Drain Station. As shown in Figure 5.

Table 17 displays the Thiessen coefficient by comparing the length of the sub-DAS with the total length of the DAS. Using the Thiessen polygon method in millimeters, Table 18 displays the average rainfall of the DAS.

The coverage area represented by each rainfall station, determined through the Thiessen Polygon method, is detailed in Table 17. These area values serve as the basis for calculating the regional average rainfall for the watershed, with the final results presented in Table 18.

The method used to determine rainfall in the Angke-Pesanggrahan watershed is the Thiessen Polygon Method. This method was chosen based on the characteristics of spatial distribution, in which each rain station has a unique and non-uniform area of influence. The analysis involved five influential rainfall stations, which are Sawangan Station, Bendung Gintung, Cengkareng Drain, Situ Parigi, and Villa Pamulang.

Table 17. Influence area values for each rain station.

No	Station Name	Area (km^2)	Thiessen coefficient
1	Cengkareng Drain	139.49	0.281
2	Bendung Gintung	57.25	0.115
3	Situ Parigi	109.69	0.221
4	Villa Pamulang	56.54	0.114
5	Sawangan	133.49	0.269
	Total	496.46	1

The process of mapping the area of influence was carried out using a working map with a scale of 1:330.000. The calculation steps began with determining the watershed boundaries at the review point, then plotting the five stations based on their geographical coordinates. Based on the results of the polygon mapping, the total Thiessen polygon influence area was 496.46 km^2. The unique area of each station was then used as a weighting factor to produce accurate rainfall design input for hydrodynamic simulation.

Probability Distribution

Probability distribution tests are used to determine whether the observed probability distribution can be used to calculate the sample data's statistical distribution under analysis. The test analysis results are shown in Tables 19 and 20 below, with the most accurate distribution being the Log Pearson III distribution.

© 2026 Dept. of Geophysics Hasanuddin University

Table 18. Rainfall values in the Angke Pesanggrahan watershed area from 2009 to 2023.

Year	Rainfall Station (mm)					
	Sawangan	Bendung Gintung	Cengkareng Drain	Situ Parigi	Villa Pamulang	Rainfall
2009	85.0	27.9	139.0	30.9	25.5	74.9
2010	108.0	24.6	75.0	27.2	22.5	61.5
2011	76.0	20.5	83.0	22.8	18.8	53.3
2012	83.4	18.6	54.0	20.6	17.0	46.2
2013	100.0	25.1	91.0	27.8	22.9	64.1
2014	100.0	26.6	105.0	29.4	24.3	68.7
2015	146.8	20.6	124.0	28.8	23.8	85.7
2016	353.4	39.1	156.5	46.7	38.5	158.2
2017	134.0	43.4	143.5	39.2	32.4	93.7
2018	202.0	27.8	108.3	31.0	14.3	96.4
2019	454.4	55.5	551.7	57.0	62.5	303.3
2020	170.7	47.0	203.5	63.1	52.8	128.4
2021	309.7	55.1	120.6	44.1	46.6	138.6
2022	331.2	50.4	162.4	56.6	47.5	158.4
2023	392.1	33.7	80.9	32.1	49.1	144.7

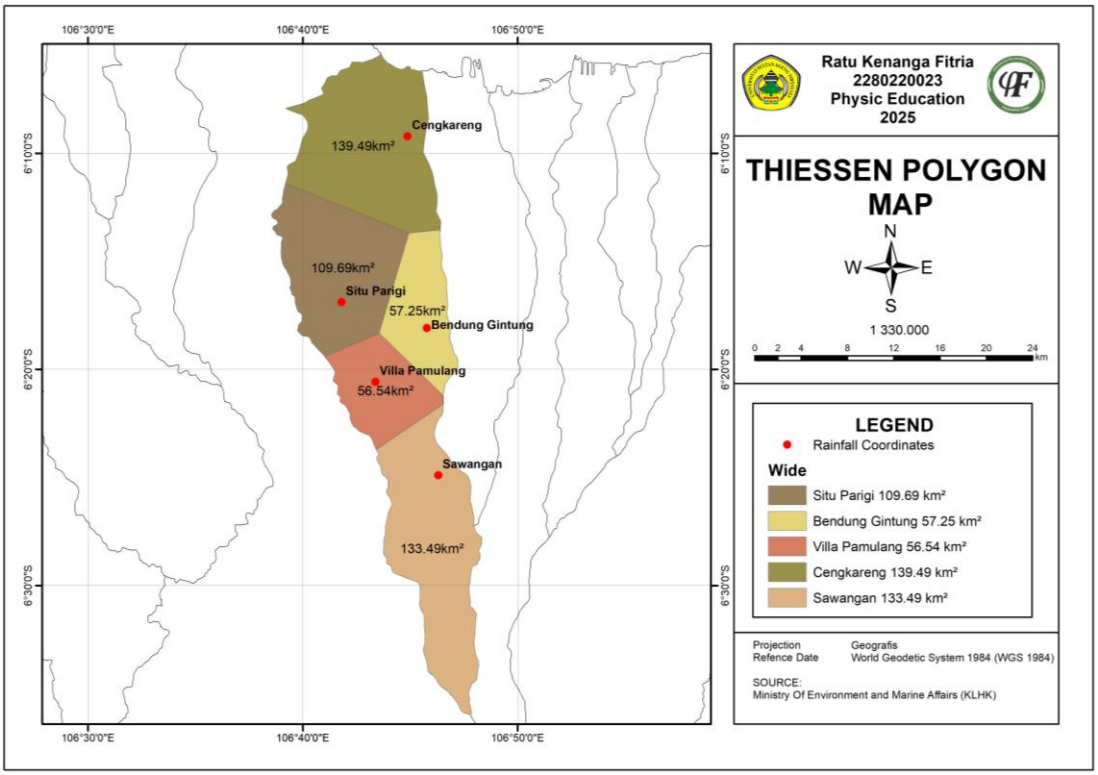

Figure 5. Map of the Angke Pesanggrahan watershed using the thiessen polygon method.

a) Chi-Square Test

Table 19. Calculation results X^2 and X^2_{cr}.

CHI-SQUARE TEST				
Description	**Distribution**			
	Gumbel	**Log Pearson**	**Normal**	**Log Normal**
X^2critis α (1%)	9.21	9.21	9.21	9.21
X^2critis α (5%)	5.991	5.991	5.991	5.991
Degrees of Freedom (DF)	2	2	2	2
X^2count	5.3	0.7	7.3	0.7
Description (1%)	Accepted	Accepted	Accepted	Accepted
Description (5%)	Accepted	Accepted	Rejected	Accepted
Difference (1%)	3.9	8.5	1.9	8.5
Difference (5%)	0.7	5.3	-1.3	5.3

© 2026 Dept. of Geophysics Hasanuddin University

b) Smirnov-Kolmogorof Test

Table 20. Distribution test calculation results using the Smirnov-Kolmogorov method.

SMIRNOV-KOLMOGOROF TEST				
Description	**Distribution**			
	Gumbel	**Log Pearson**	**Normal**	**Log Normal**
Δcritical α (1%)	0.4	0.4	0.4	0.4
Δcritical α (5%)	0.34	0.34	0.34	0.34
Large data (n)	15	15	15	15
Δcount	0.13	0.11	0.15	0.08
Description (1%)	Accepted	Accepted	Accepted	Accepted
Description (5%)	Accepted	Accepted	Accepted	Accepted
Difference (1%)	0.273	0.29	0.246	0.317
Difference (5%)	0.213	0.23	0.186	0.257

Table 21. Planned rainfall calculation results.

Repeatability [Tr] (Year)	Pr (%)	K	$K.Sd_{Log\ R}$	Log R_{design}	R_{design} (mm)
2	50	-0.141	-0.0313	1.961	88.26
5	20	0.774	0.1712	2.163	122.12
10	10	1.338	0.2960	2.288	149.20
25	4	2.008	0.4442	2.436	189.25
50	2	2.479	0.5485	2.540	223.71
100	1	2.930	0.6481	2.640	262.48
200	0.5	3.364	0.7442	2.736	306.23
1000	0.1	4.328	0.9574	2.949	431.12

Rainfall Analysis Plan

Based on the frequency analysis using Equation (1), the planned rainfall values were obtained. These results, representing the Log Pearson Type III distribution, are presented in Table 21.

Planned flood discharge

Planned flood discharge based on Equation 3 above, the planned discharge was obtained using the Nakayasu HSS method. Table 22 below shows the results obtained.

Table 22. Planned flood discharge calculation results.

No	Repeatability [Tr] (Year)	Planned Flood Discharge (m^3/s)
1	2	296.9
2	5	473.1
3	10	630.7
4	25	887.2
5	50	1128
6	100	1418.8
7	200	1770.2
8	1000	2892.3

The final estimation of peak flood discharges for various return periods, based on the integrated hydrological modelling, is summarized in Table 23. These values serve as the primary input for the subsequent flood inundation mapping.

The hydrological data used in this study consist of annual peak flood discharge records. The fluctuation and distribution of these discharge values over the observation period, which serve as the primary input for the frequency analysis, are presented in Figure 6.

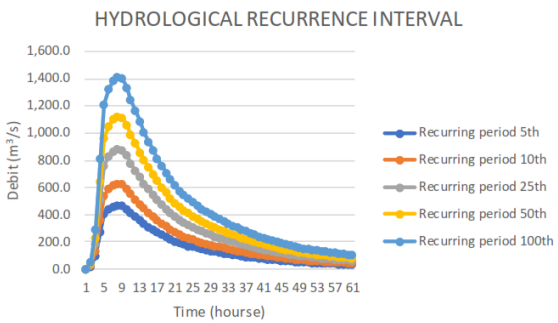

Figure 6. Total Runoff Hydrograph for 5, 10, 25, 50, and 100-year return periods, Nakayasu HSS.

Sensitivity analysis on the Nakayasu HSS model was conducted to identify the extent to which the flow coefficient (C) and peak time (T_p) parameters affect the design flood discharge in the Angke-Pesanggrahan watershed. The simulation results show that

© 2026 Dept. of Geophysics Hasanuddin University

variations in these parameter values significantly affect the hydrograph elevation, where the peak discharge (Q_{50}) produced reaches 1127.97 m^3/s. This value was then validated numerically through direct comparison with the existing storage capacity on the Cengkareng River section (Reach 4) using the HEC-RAS program. The results of ArcGIS and RAS Mapper mapping, showing the accumulation of unaccommodated discharge, are visualized in Figure 7.

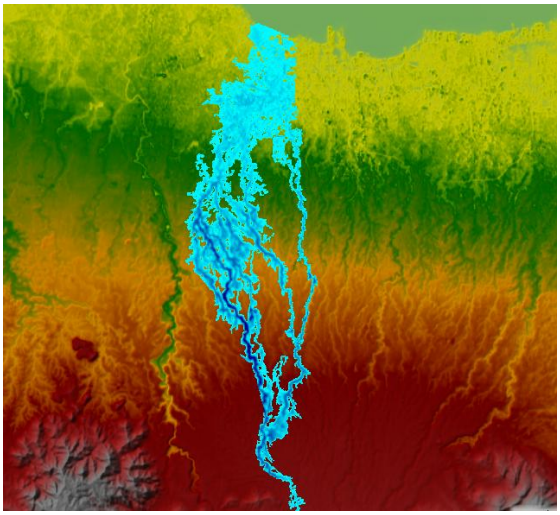

Figure 7. Results of 50-year flood modelling.

Table 23. Results of river cross-section analysis (existing) using the HEC-RAS program.

River	Location Name	Flood Discharge (m^3/s)	River Capacity (m^3/s)	Description
1	Kembangan Utara	1128	599.78	not safe
2	Kedaung Kali Angke	1128	592.12	not safe
3	Kapuk Muara	1128	565.41	not safe
4	Kamal Muara	1128	565.00	not safe
5	Cengkareng Timur	1128	596.47	not safe
6	Kedoya Utara	1128	598.54	not safe

Explanation:
Safe: flood discharge < river capacity
Not safe: flood discharge > river capacity

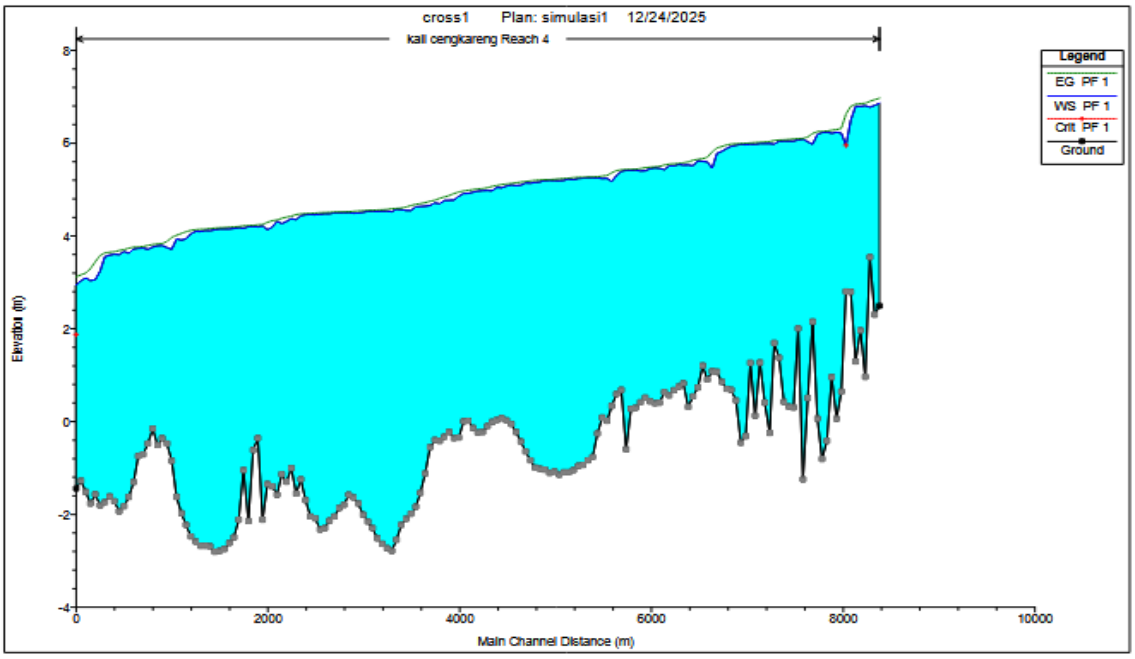

Figure 8. Longitudinal profile of the Cengkareng river.

The hydraulic simulation results for the 50-year return period (Q_{50}) are visualized through the cross-sectional profiles in Figure 8 – 11. The analysis indicates that the existing river capacity is insufficient to accommodate the peak discharge of 1.128 m^3/s. As illustrated in these figures, the water level (represented by the blue area) significantly exceeds the main channel's bank stations (marked by the red dots),

© 2026 Dept. of Geophysics Hasanuddin University

particularly in the downstream sections. This overflow confirms that the river has reached its maximum capacity, leading to extensive flooding in the surrounding areas due to the water overtopping the riverbanks.

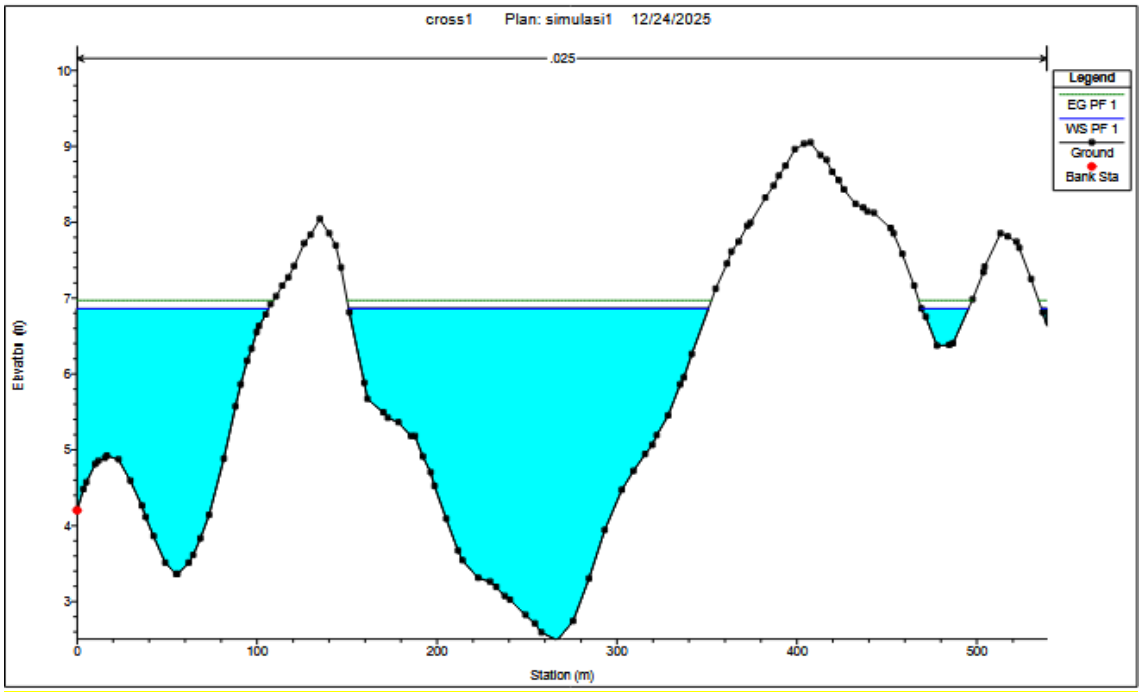

Figure 9. Cross-section of the Cengkareng river at the headwaters.

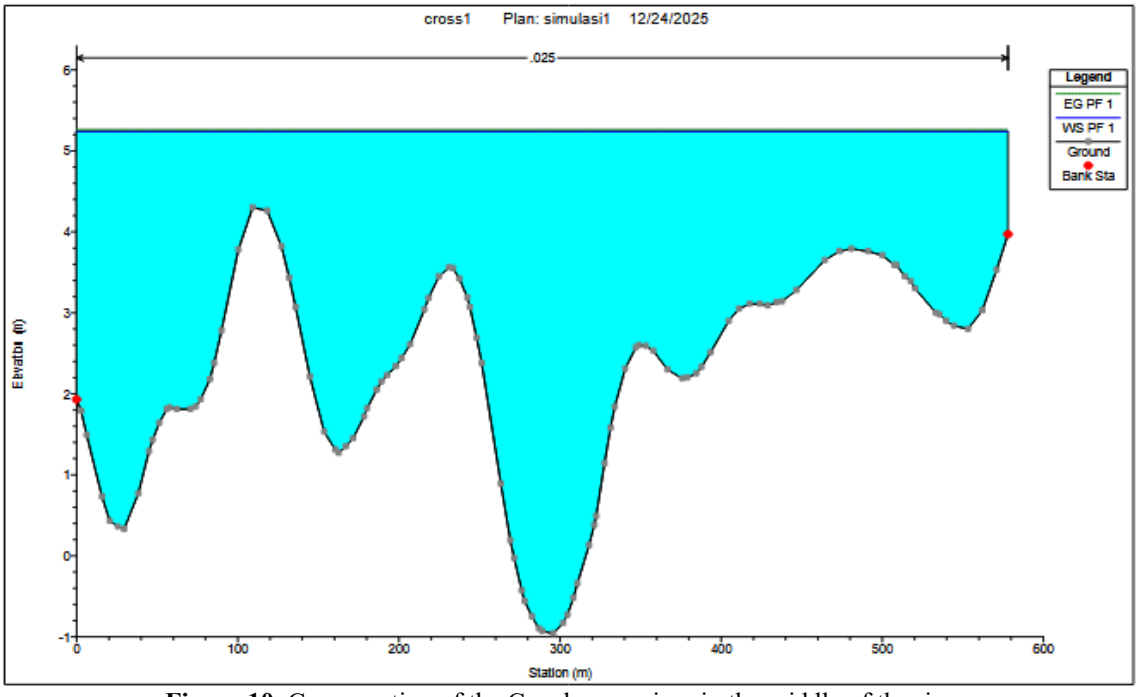

Figure 10. Cross-section of the Cengkareng river in the middle of the river.

© 2026 Dept. of Geophysics Hasanuddin University

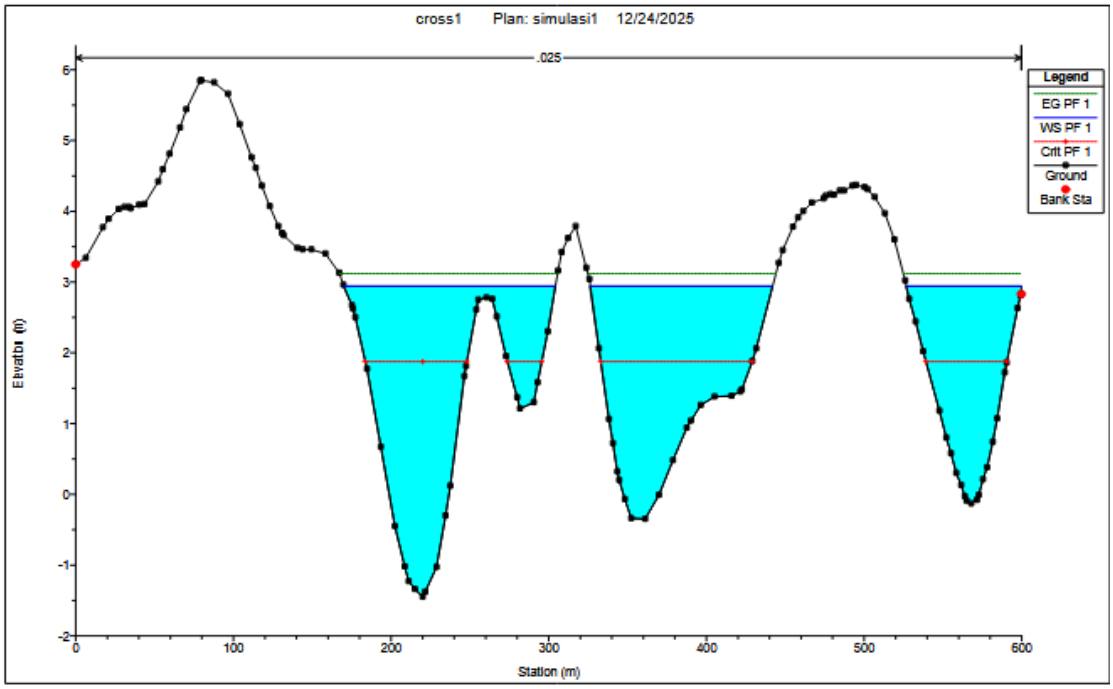

Figure 11. Cross-section of the Cengkareng river at the downstream section.

The flood vulnerability analysis in this study integrates hydrological sensitivity parameters through Nakayasu HSS method and hydrodynamic simulation using HEC-RAS 6.7. Sensitivity analysis in Nakayasu's modelling was conducted to determine the peak discharge based on various return periods. The calculation results show that for a 50-year return period (Q_{50}), the design flood discharge reaches 1128 m^3/s. This figure was validated through the Hydrological Recurrence Interval graph, which shows a very significant peak discharge surge compared to the recurrence periods below it. Numerical validation of river safety levels was carried out by comparing the design flood discharge (Q_{50}) with the river capacity at six critical locations along the Cengkareng River (Figure 8 – 11). The comparison results show that the current river capacity ranges from only 565 to 599.78 m^3/s. The comparison graph of planned discharge vs. river capacity (Figure 12) visually emphasizes the 'Not Safe' condition, where the planned flood discharge exceeds the river capacity by almost double at each observation location. This condition was confirmed technically through cross-section modelling in the upstream, middle, and downstream sections of the river. HEC-RAS simulations show that the water level at Q_{50} conditions has exceeded the elevation of the river banks (bank stations), resulting in massive flooding in the surrounding areas. Spatially, the results of ArcGIS and RAS Mapper mapping (Figure 7) show that this unaccommodated discharge accumulation spread to densely populated residential areas downstream with varying flood depths, providing strong quantitative and visual evidence for the need for immediate structural mitigation efforts.

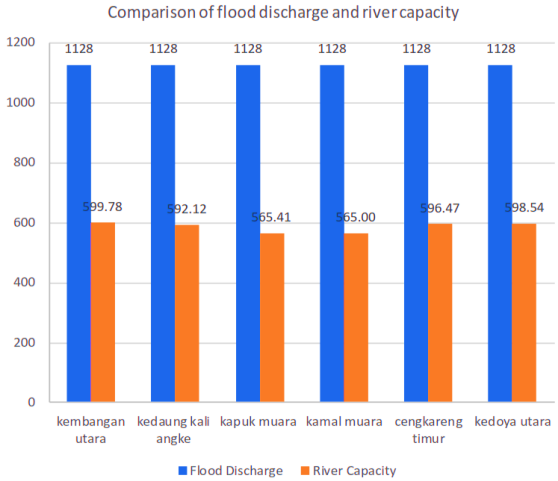

Figure 12. Comparison of flood discharge and river capacity.

© 2026 Dept. of Geophysics Hasanuddin University

Flood-Prone Areas

The analysis of flood-prone areas in the Angke-Pesanggrahan watershed was conducted through the integration of GIS technology with the overlay scoring method based on the Analytic Hierarchy Process (AHP), an approach that, according to Monir et al. (2026), is highly effective in combining multidimensional geospatial data with measurable assessment consistency through the Consistency Ratio (CR). Physical parameters of the area were validated using the pairwise comparison method and visualized in a Flood Risk Map (Figure 13), which served as a crucial validation tool to confirm the accuracy of the HEC-RAS hydrodynamic simulation results on the Cengkareng River section. The use of this hybrid model strengthens the reliability of spatial mapping, ensuring that the resulting risk zoning is in line with field conditions and can serve as a strong scientific basis in supporting disaster management policies and adaptive spatial planning.

The mapping results show a strong linear correlation with the numerical findings in the HEC-RAS model. The downstream area, particularly around the Cengkareng River, which covers the areas of Kembangan Utara, Kedaung Kali Angke, Kapuk Muara, Kamal Muara, Cengkareng Timur, and Kedoya Utara, is classified as "Vulnerable" to "Very Vulnerable." Technically, the very high vulnerability status in ArcGIS validates the field conditions where the numerical river capacity (average 596 m^3/s) proved unable to accommodate the planned flood discharge (Q_{50}) of 1128 m^3/s.

The inability of the river to accommodate the discharge caused water to accumulate and overflow the levees, which was spatially mapped as extensive flooding in densely populated settlements. Thus, this vulnerability map is not merely a statistical representation, but rather visual evidence that is synchronized with the river's hydraulic failure found in the HEC-RAS simulation. The integration of these two methods ensures that the identified flood hotspots are highly accurate because they are based on multifactorial GIS parameters and validated by extreme water flow dynamics.

From Figure 13, detailed spatial distributions for each vulnerability category, ranging from safe to highly prone areas, are shown in Figures 14 – 17.

The accuracy of this mapping was confirmed in downstream areas such as Cengkareng, Kembangan, and Kebon Jeruk (Highly Vulnerable Areas Map in Figure 17), where the water surface elevation (W.S. Elev) reached 4.15 m. These results show a high level of precision between the spatial and numerical models, the areas identified as having the highest vulnerability scores in GIS consistently coincide with the overtopping points in the HEC-RAS simulation, which have a flood width (Top Width) of up to 566.99 m.

Using the actual discharge value of 1.128 m^3/s as a validation instrument, this vulnerability map has strong scientific validity. The "Highly Vulnerable" status in coastal and downstream areas (Highly Vulnerable Map) is supported by comparative numerical data (Figure 17) showing a "Not Safe" status across all observation locations. This proves that the map produced is an accurate reflection of the physical dynamics of flooding in the field.

© 2026 Dept. of Geophysics Hasanuddin University

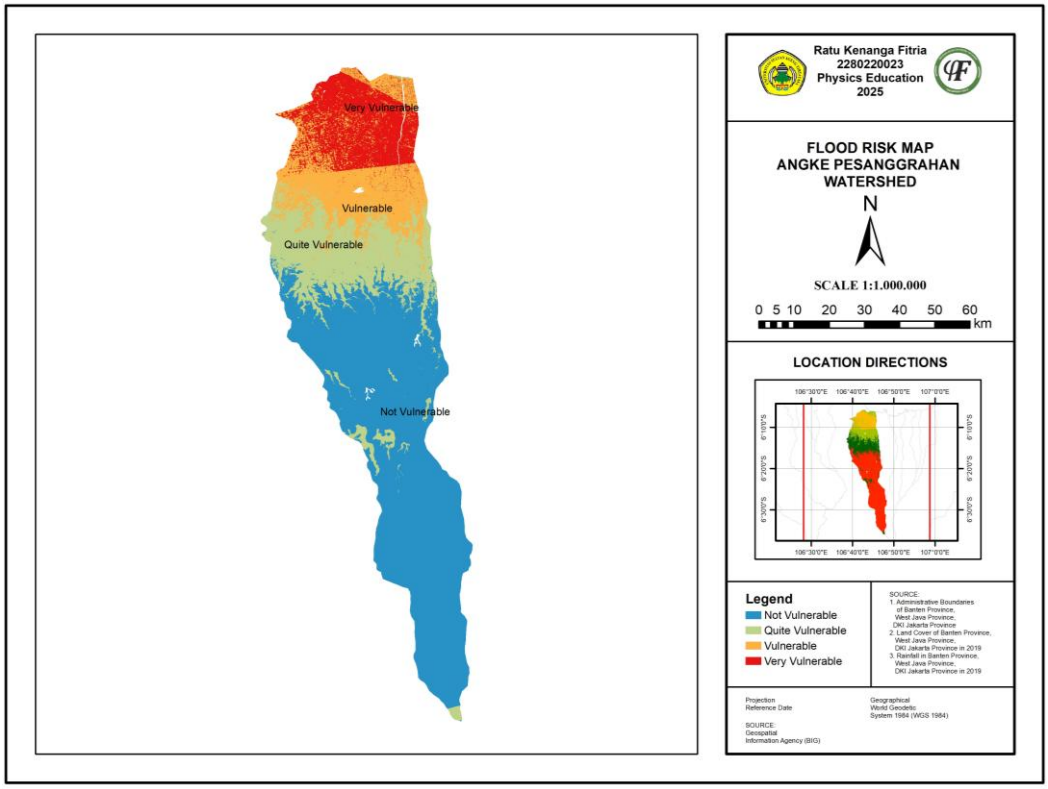

Figure 13. Angke Pesanggrahan watershed flood prone map.

The accuracy of these modeling results is strongly supported by records of actual flooding events in the downstream area of the Angke-Pesanggrahan watershed. Based on disaster reports, the areas of South Kedoya, Kebon Jeruk, and Kembangan consistently experience severe flooding when extreme rainfall hits Greater Jakarta. For example, the extreme flood event in January 2020, triggered by record-breaking rainfall intensity, caused widespread inundation across Jakarta with water levels reaching critical heights in areas such as Kembangan due to the overflow of the Pesanggrahan river system (Dahlia & Fadiarman, 2020). This incident validates the HEC-RAS simulation results in this study, which show that the water surface elevation (W.S. Elev) is at a critical level of 4.15 m and the storage capacity is 'Not Safe'.

In addition, data from the Jakarta Regional Disaster Management Agency (BPBD) (BPBD, 2021) noted that the Cengkareng and Penjaringan areas were prone to flooding with long receding times. This is in line with the 'Very Vulnerable' classification on the ArcGIS vulnerability map (Figure 13) and the spatial modeling results, which showed that the widest accumulation of flooding was in these areas. The consistency between media/field data and the results of this numerical modeling proves that the integration of the Nakayasu HSS, HEC-RAS, and GIS methods in this study has a very high level of accuracy in representing the actual flood risk in the field.

© 2026 Dept. of Geophysics Hasanuddin University

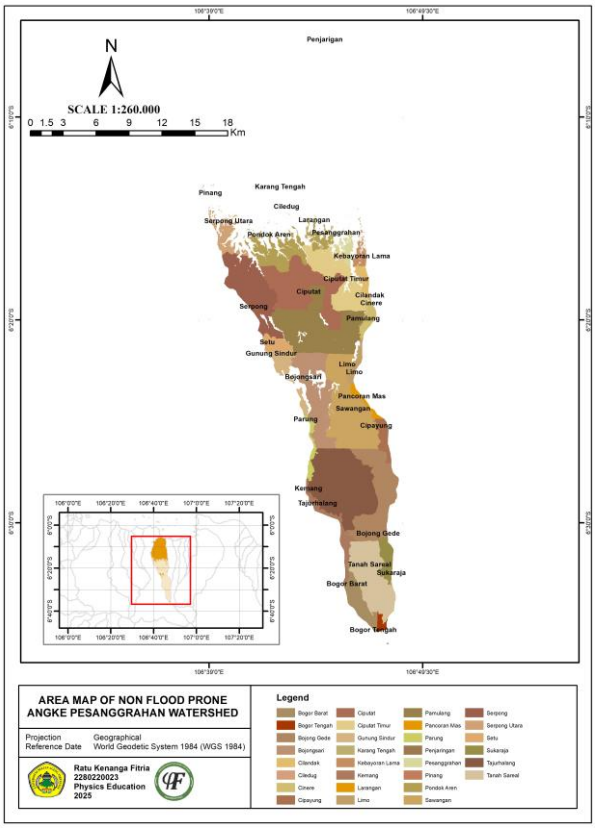

Figure 14. Map of non-flood prone areas.

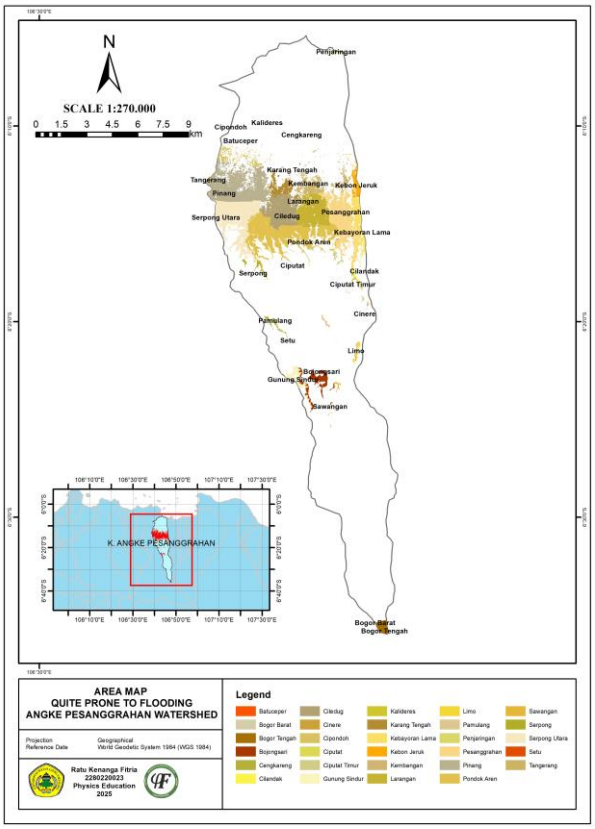

Figure 15. Map of quite prone areas.

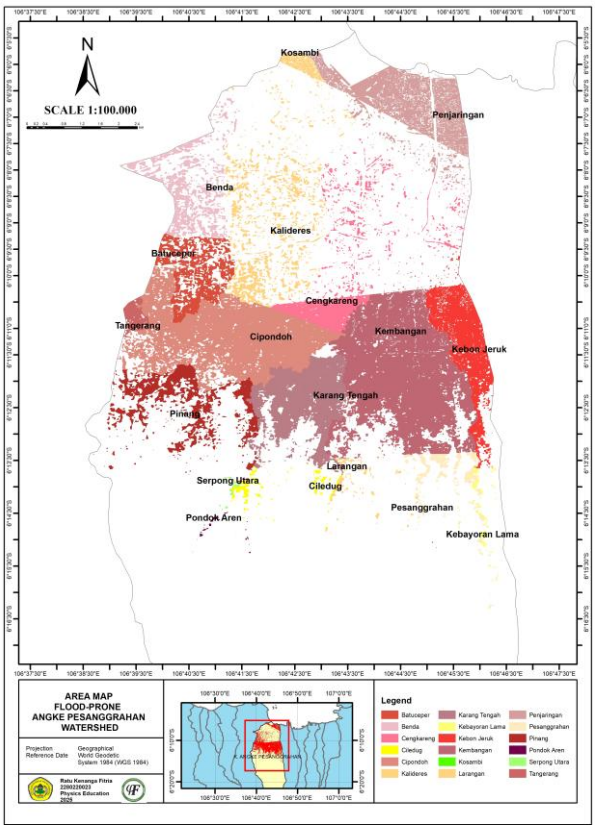

Figure 16. Map of flood-prone areas.

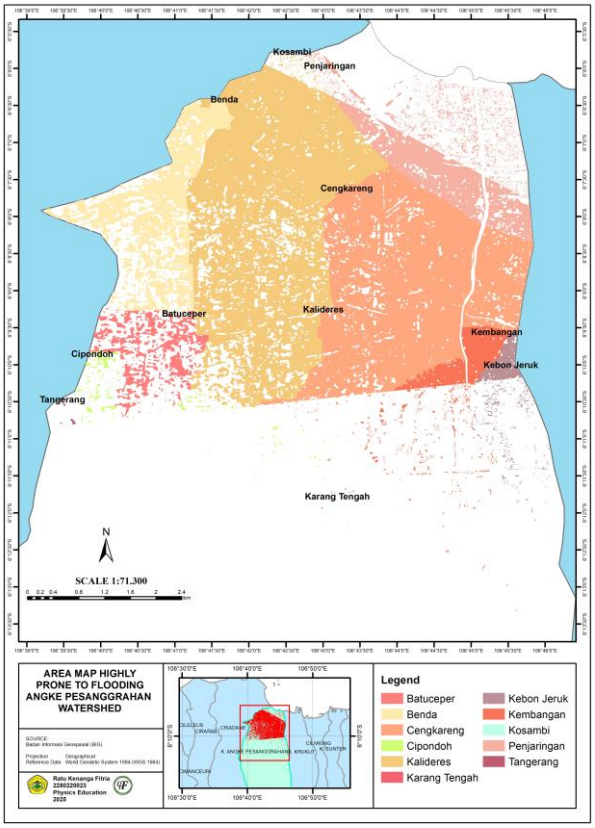

Figure 17. Map of highly prone areas.

© 2026 Dept. of Geophysics Hasanuddin University

Conclusion

Based on a series of systematic analyses using the Thiessen Polygon method, Log Pearson Type III distribution, and Nakayasu HSS, the capacity of the Cengkareng River downstream of the Angke-Pesanggrahan watershed is deemed inadequate due to its critical condition. The simulation results show that the design flood discharge (Q_{50}) reaches 1127.97 m^3/s, a figure that significantly exceeds the river's numerical storage capacity, which ranges from only 565 to 599.78 m^3/s. The inadequacy of this cross-section is validated by the HEC-RAS model with a water level elevation of 4.15 m and a flood width of 566.99 m, which spatially confirms the "Very Vulnerable" zone in the Kembangan Utara, Kedaung Kali Angke, Kapuk Muara, Kamal Muara, Cengkareng Timur, Kedoya Utara areas as mapped in ArcGIS and supported by historical flood data records.

As a mitigation measure, it is necessary to integrate short-term structural solutions in the form of normalization and elevation of embankments at critical points with a "Not Safe" status to prevent overtopping, as well as riverbank management through the relocation of residents in the "Very Vulnerable" zone. Non-structurally, long-term sustainability must be pursued through the restoration of soil infiltration functions by planting vegetation and constructing infiltration wells to reduce surface runoff. Given that this study is limited to numerical simulations, future studies are recommended to integrate inflow variables from tributaries and the impact of sedimentation, which has the potential to reduce the effective capacity of rivers more drastically.

Acknowledgements

We would like to thank the Ciliwung-Cisadane River Basin Agency (BBWS) and the Geospatial Information Agency (BIG) for providing secondary data in the research process, enabling this paper to become useful information for the community. We would also like to thank the lecturers who have provided a lot of input.

Author Contribution

Ratu Kenanga Fitria contributed to conceptualization, data curation, formal analysis, investigation, project administration, software development, visualization, writing-original draft preparration, and writing-review & editing. Yayat Ruhiat was responsible for methodology, resources, supervision, and validation. Yuvita Oktarisa contributed to supervision and validation.

Conflict of Interest

The authors declare no conflict of interest.

References

Abdolazimi, O., Sepehrifar, M., Shishebori, D., Banicescu, I., Azad, S., Pishini, K., & Ma, J. (2025). A stochastic DEA-GARMA integration for dynamic forecasting of undesirable outputs applied to the temporal efficiency analysis of water and sewerage services. *Journal of Cleaner Production*, 521(146177). https://doi.org/10.1016/j.jclepro.2025.146177

Alif, M. S. A., Marma, M-E-S., Hassan, M. N., Jahan, C. S., Howlader, R., Sarker, T., Rasel, M. I. A., Mahim, M. M. A., Roy, R., & Mazumdar, Q. H. (2025). Flash flood risk zoning in Gomti River Basin in Eastern Bangladesh and Tripura State (India) using MCDM-GIS Tool. *Safety in Extreme Environments*, 7,7. https://doi.org/10.1007/s42797-025-00120-7

Allafta, H., & Opp, C. (2021). GIS-based multi-criteria analysis for flood prone areas mapping in the trans-boundary

© 2026 Dept. of Geophysics Hasanuddin University

Shatt Al-Arab basin, Iraq-Iran. *Geomatics, Natural Hazards and Risk*, 12(1), 2087–2116. https://doi.org/10.1080/19475705.2021.1955755

Bahago, R. A., Abdulkadir, A., Yahaya, T. I., & Hassan, A. B. (2026). Geospatial Assessment of Flood Vulnerability and Its Impact on Food Security in Downstream Communities of Shiroro and Zungeru Dams, Niger. *Research Square* [Preprint], 0–23.

BPBD. (2021). *Data Titik Genangan dan Banjir Provinsi DKI Jakarta Tahun 2020-2021*. BPBD DKI Jakarta.

Carr, G., Seebauer, S., & Lun, D. (2025). Interactions Between Public and Private Flood Adaptation: Insights from a Socio – Hydrological Model. *Water Resources Research*, 61, e2025WR040502. https://doi.org/10.1029/2025WR040502

Dahlia, S., & Fadiarman. (2020). Analisis risiko banjir terhadap fasilitas pendidikan di DKI Jakarta. *Jurnal Geografi Gea*, 20(2), 185–196. https://doi.org/10.17509/gea.v20i2.24113

Endendijk, T., Botzen, W. J. W., de Moel, H., Aerts, J. C. J. H., Slager, K., & Kok, M. (2023). Flood vulnerability models and household flood damage mitigation measures: An econometric analysis of survey data. *Water Resources Research*, 59, e2022WR034192. https://doi.org/10.1029/2022WR034192

Fox, S., Agyemang, F., Hawker, L., & Neal, J. (2024). Integrating social vulnerability into high- resolution global flood risk mapping. *Nature Communications*, 15, 3155. https://doi.org/10.1038/s41467-024-47394-2

Glas, R., Hecht, J., Simonson, A., Gazoorian, C., & Schubert, C. (2023). Adjusting design floods for urbanization across groundwater-dominated watersheds of Long Island, NY. *Journal of Hydrology*, 618, 129194. https://doi.org/10.1016/j.jhydrol.2023.129194

Guo, J., Meng, Q., Du, B., & Sun, H. (2025). Probability forecasting for multivariate urban water demand using temporal convolutional network based on quantile regression and Parzen window. *Engineering Applications of Artificial Intelligence*, 162, 112528. https://doi.org/10.1016/j.engappai.2025.112528

Habibi, N. I., & Darmawan, Y. (2024). Pengendalian Banjir Pada Daerah Aliran Sungai Pesanggrahan Menggunakan Pemodelan HEC-RAS. *Jagratara: Journal of Disaster Research*, 2(2), 27–36. https://doi.org/10.36080/jjdr.v2i1.146

Handore, K. R., Patil, N., & Dangle, M. (2025). Comparative Analysis of Disaster Management Strategies in India and Indonesia. *Indonesian Journal of Geography*, 57(3), 480–494. https://doi.org/10.22146/ijg.101454

Ignes, J., & Arbaningrum, R. (2021). Analisis Debit Maksimum pada Long Storage Sungai Serua di Lingkungan Universitas Pembangunan Jaya. *Jurnal Proyek Teknik Sipil*, 4(2), 43–48. https://doi.org/10.14710/potensi.2021.11540

Ismael, Y. M., & Awchi, T. A. (2023). Meteorological Drought Analysis in Iraq using SPI and Theory of Runs for the Period 1980-2022. *IOP Conference Series: Earth and Environmental Science*, 1374, 012063. https://doi.org/10.1088/1755-1315/1374/1/012063

Kwak, J., Kim, J., Lee, H., Kim, S., Kim, S., & Seong, M. (2024). Evaluation of future flood probability in agricultural reservoir watersheds using an integrated flood simulation system. *Journal of Hydrology*, 628, 130463.

© 2026 Dept. of Geophysics Hasanuddin University

https://doi.org/10.1016/j.jhydrol.2023.130463

Limeria, A. & Saputra, R. H. (2024). Penentuan Debit Banjir Dengan HEC-HMS dan Kawasan Rawan Banjir Dipengaruhi Pasang Surut Dengan HEC-RAS 2D. *Jurnal Teknika: Jurnal Teoritis dan Terapan Bidang Keteknikan*, 7(2), 14–20. https://e-journal.upr.ac.id/index.php/JT/article/view/14077

Mester, B., Fieler, K., Korup, O., Desai, B., & Schewe, J. (2025). Socioeconomic predictors of vulnerability to flood-induced displacement. *Nature Communications*, 16, 8296. https://doi.org/10.1038/s41467-025-64015-8

Mitu, M. F., Sofia, G., & Anagnostou, E. N. (2025). Using Flood Insurance Claims in Coastal CONUS to Evaluate the Impact of Compound Flood Risk. *Water Resources Research*, 61, e2024WR039384. https://doi.org/10.1029/2024WR039384

Monir, M., Sarker, S. C., & Akhter, S. (2026). Participatory flood vulnerability assessment in the Teesta floodplain of Bangladesh using GIS-based AHP and frequency ratio models. *Next Sustainability*, 7, 100251. https://doi.org/10.1016/j.nxsust.2026.100251

Muhammad, I. N., Sarpono, S., Wibowo, A., Rachmat, S., & Kurniadi, A. (2025). Spatial Analysis of Urban Flood Vulnerability Using Weighted Overlay Technique for Identification of Hazard Zones in Greater Jakarta. *Jurnal Geografi*, 23(1), 223–238. https://doi.org/10.26740/jggp.v23n1.p223-238

Novarini, N., Harahap, A. K., Syastra, M. T., Yulia, I., Sutrisno, S., & Wijayanti, E. K. (2024). Sistem Informasi Geografis Bencana Alam Banjir Jakarta Berbasis Web dengan Metode SDLC. *Jurnal Informatika Teknologi dan Sains (Jinteks)*, 4(4), 489–495. https://doi.org/10.51401/jinteks.v4i4.4752

Noviansah, W. (2025). *Banjir 3,5 Meter Rendam Pesanggrahan Jaksel, 400 Warga Dievakuasi*. DetikNews. https://news.detik.com/berita/d-7806531/banjir-3-5-meter-rendam-pesanggrahan-jaksel-400-warga-dievakuasi

PSDA WS Ciliwung-Cisadane. (2019). *Data Curah Hujan (mm).*

PSDA WS Ciliwung-Cisadane. (2023). *Data Curah Hujan (mm).*

Rahmadani, S., Harahap, R., & Pongtuluran, E. H. (2023). Evaluasi Pola Distribusi Stasiun Hujan Kota Medan. *Jurnal Teknik Hidraulik Atau Jurnal Konstruksia*, 9(1), 10–19. https://jurnal.poltekba.ac.id/index.php/jst/article/view/1737

Rahmadani, S., Harahap, R., Yuzni, S. Z., Rani, C. M., Tinov, N., Waruwu, J. A., & Rahmadani, S. S. (2024). Hydrological Study of Deli River Flood Discharge Using the HSS Nakayasu Model. *Journal of Physics: Conference Series*, 2908, 012016. https://doi.org/10.1088/1742-6596/2908/1/012016

Rhianazala, A., Budiyanto, M. N., & Iriani, A. (2026). Analyzing the Challenges of Flood Management Policies in Bekasi City through Target Mapping Techniques. *Jurnal Pemerintahan Dan Politik*, 11(1), 108–133. https://ejournal.uigm.ac.id/index.php/PDP/article/view/5951

Saad, M. S. H., Ali, M. I., Razi, P. Z., Ramli, N. I., & Jaya, R. P. (2024). Exploring the Factors and Impacts of Flash Floods Vulnerability in Various Areas of Malaysia: A Content Analysis. *Disaster in Civil Engineering and Architecture*, 1(1), 55–82. https://doi.org/10.70028/dcea.v1i1.11

Safaei-Moghadam, A., Hosseinzadeh, A., & Minsker, B. (2024). Predicting real-time roadway pluvial flood risk: A hybrid machine learning approach

© 2026 Dept. of Geophysics Hasanuddin University

coupling a graph-based flood spreading model, historical vulnerabilities, and Waze data. *Journal of Hydrology*, 637, 131406. https://doi.org/10.1016/j.jhydrol.2024.131406

Saraswati, Y., Arifin, A., & Irsan, R. (2023). Pemetaan Sebaran Tempat Penampungan Sampah Sementara (TPS) di Kecamatan Sintang menggunakan Sistem Informasi Geografis (SIG). *Jurnal Ilmu Lingkungan*, 21(2), 238–244. https://ejournal.undip.ac.id/index.php/ilmulingkungan/article/view/45522

Setiyawan, S., Vera, W. A., Irdhiani, I., Rehana, R., Sri, H., & Hasbi, A. (2022). Testing of The Method of Gama I Synthetic Unit Hydrograph in The Analysis of The Tojo Watershed Design Flood. *IOP Conference Series: Earth and Environmental Science*, 1075, 012050. https://doi.org/10.1088/1755-1315/1075/1/012050

Sinurat, M., Mulia, A. P., & Faisal, M. (2022). Analisis spasial daerah banjir menggunakan HEC-RAS dan QGIS untuk Sub DAS Babura. *Jurnal Syntax Admiration*, 3(1), 141–162. https://doi.org/10.46799/jsa.v3i1.382

Soma, A., Arsyad, U., Nursaputra, M, Lando, A. T., Rahmat, S., Azus, F. H., & Ramadhan, M. D. R. (2021). Flood vulnerability analysis using the frequency ratio method with the watershed ecosystem in Bulukumba Regency, South Sulawesi Indonesia. *IOP Conference Series: Earth and Environmental Science*, 1230, 012044. https://doi.org/10.1088/1755-1315/1230/1/012044

Syukur, R. E. R. (2025). *Ruas jalan di Kembangan banjir akibat Kali Pesanggrahan meluap*. Antara News. https://www.antaranews.com/berita/4686793/ruas-jalan-di-kembangan-banjir-akibat-kali-pesanggrahan-meluap

Taki, H. M., & Wartaman, A. S. (2022). Study of Flood Vulnerability in Pesanggrahan District, South Jakarta. *Journal of Applied Geospatial Information*, 6(2), 647–651. https://doi.org/10.30871/jagi.v6i2.4308

Wigati, R., & Wahyudin, W. (2013). Analisis Banjir Sungai Ciliwung (Studi Kasus Ruas Sungai Lenteng Agung-Manggarai). *Fondasi : Jurnal Teknik Sipil*, 2(1), 1–9. https://doi.org/10.36055/jft.v2i1.1985

Yu, J., Wang, G., Yinglan, A., Zhu, Y., Cheng, Y., Deng, Z., Gao, R., & Duan, L. (2025). Hydrological phase-driven management in semi-arid watersheds: Linking plankton assembly dynamics and adaptive resilience strategies. *Water Research X*, 29, 100421. https://doi.org/10.1016/j.wroa.2025.100421

© 2026 Dept. of Geophysics Hasanuddin University